

## Observation of strong soft-x-ray amplification at 8.8 nm in the transient collisional-excitation scheme

Tetsuya Kawachi, Akira Sasaki, Momoko Tanaka, Maki Kishimoto, Noboru Hasegawa, Keisuke Nagashima, Masato Koike, Hiroyuki Daido, and Yoshiaki Kato

*Advanced Photon Research Center, Kansai-Research Establishment, Japan Atomic Energy Research Institute, 8-1, Umemidai, Kizu, Kyoto 616-0215, Japan*

(Received 8 August 2002; revised manuscript received 30 July 2003; published 5 March 2004)

We have observed strong amplification with a gain of  $14.5 \text{ cm}^{-1}$  for the  $4d \rightarrow 4p$  transition of the Ni-like La ions at a wavelength of 8.8 nm pumped by a chirped pulse amplification Nd:glass laser with an energy of 18 J. In this experiment, the laser pulses consist of a prepulse and a main pulse with durations of 200 ps and 7 ps, separated by 250 ps. The keV x-ray spectroscopy and theoretical calculation indicate that the plasma temperature increased effectively by reducing the prepulse intensity, and that the substantial gain is generated in a small overcritical region heated by the electron heat transport.

DOI: 10.1103/PhysRevA.69.033805

PACS number(s): 42.55.Vc, 42.60.By, 52.50.Jm

Development of high brightness compact x-ray sources is an important subject for the applications in various research fields such as material science, biological science, and atomic and molecular physics. X-ray lasers, which have characteristics such as high spatial coherence and high peak brilliance, have been one of the promising compact x-ray sources, and continuous efforts have been made to realize highly efficient intense x-ray output. Recently the transient collisional excitation (TCE) scheme has been proposed [1], and now we can obtain the gain saturation of the Ni-like ion lasers in a wavelength region up to 12 nm with a pumping energy of  $\sim 10 \text{ J}$  [2–4], which is only a few 10% of that in the quasi-steady-state (QSS) collisional excitation lasers [5]. In a shorter wavelength region than 10 nm, however, TCE scheme is not optimized sufficiently: substantial amplification of the Ni-like Sm TCE laser at 7.3 nm still requires more than 50 J pumping energy [6], although the gain saturation is achieved with a pumping energy of 75 J in the QSS scheme [7]. Because shorter wavelength x-ray lasers expand the applicable research fields such as time-resolved measurement of speckles from various materials with higher spatial resolution [8] and single-shot x-ray imaging of biological cell [9], it is an imminent subject to optimize the condition of the gain medium and to realize highly efficient intense x-ray lasers in the shorter wavelength region.

In the Ni-like x-ray lasers with the wavelengths of  $\sim 12 \text{ nm}$ , the optimum electron density,  $n_e$ , of the gain region is in an underdense region, and the substantial gains are generated by double pumping pulses separated by 1–2 ns [5,10,11]: The prepulse forms a preformed plasma with a long scale length, and the following main pulse heats the underdense region effectively to generate the gain. Since the collisional rate  $C$  and spontaneous radiation probability  $A$  for ions with an effective nuclear charge  $z_{\text{eff}}$  scale as  $C \propto z_{\text{eff}}^{-3}$  and  $A \propto z_{\text{eff}}^4$ , respectively, the electron temperature and density for the optimum gain condition approximately scale as  $T_e \propto z_{\text{eff}}^2$  and  $n_e \propto z_{\text{eff}}^7$ , respectively, where  $z_{\text{eff}}$  is  $z-28$  for the Ni-like ions [12,13]. This indicates that in shorter wavelength x-ray lasers, the optimum condition is expected in the high temperature and dense region. For an example, the optimum

plasma parameters for the Ni-like La ( $z=57$ ) laser at 8.8 nm [14] estimated from the typical parameters of the Ni-like Ag laser ( $T_e \sim 400 \text{ eV}$ ,  $n_e \sim 4 \times 10^{20} \text{ cm}^{-3}$ ) are inferred to be  $T_e \sim 900 \text{ eV}$  and  $n_e \sim 8 \times 10^{21} \text{ cm}^{-3}$ , which is higher than the critical density of a pumping laser pulse at a wavelength of  $1 \text{ }\mu\text{m}$ .

In order to provide the pumping energy to high-density region, frequency doubled pumping laser,  $2\omega$ , has been used [15]. However, the frequency conversion of a few ps laser pulse with an energy of  $\sim 15 \text{ J}$  needs a large-size nonlinear medium, and its low conversion efficiency ( $\sim 50\%$ ) requires a large amount of energy for the fundamental light, which is not practical and contradicts the concept of table-top x-ray lasers. Rather, it is realistic for our objective to optimize the preformed plasma condition to achieve effective heating of the high-density region by the fundamental laser light. Although the fundamental laser light cannot penetrate the overdense plasma, the laser energy absorbed near the critical density can be delivered to the high-density region by the electron thermal conduction. Since the laser energy per unit area,  $E_{\text{laser}}$ , is mainly deposited within a depth [or scale length ( $L$ )] near the critical density ( $n_C$ ), the achieved electron temperature can be approximately expressed as  $T_e \sim E_{\text{laser}}/n_C L$ , which implies that a plasma with short scale length is advantageous in terms of efficient heating. This can be understood from the increase of thermal conductivity as  $T_e^{5/2}$ . Once the critical density region becomes hot enough, the overdense region closely behind can be heated to a temperature required for the substantial production of the Ni-like ions and the population inversion.

In this paper, we show experimentally and theoretically that substantial gain can be obtained at a wavelength of 8.8 nm in the TCE scheme by reducing the prepulse intensity, where the scale length of the preformed plasma becomes short enough to obtain the plasma temperature of keV in the overdense region.

Our chirped pulse amplification pumping laser at a wavelength of  $1.053 \text{ }\mu\text{m}$  consisted of a Ti:sapphire oscillator, a pulse stretcher, a regenerative amplifier and amplifier chains of phosphate glass rods set on the optical bench with a di-

mension of  $1.2\text{ m} \times 9.0\text{ m}$ , and a pulse compressor. The details of our pumping laser and experimental setup have been described elsewhere [4,16]. A  $2\text{-}\mu\text{m}$ -thick La slab target fabricated on a  $1\text{ nm}$ -thick glass substrate was irradiated by a line-focused pumping laser light. The length and the width of the line focus were  $5.3\text{ mm}$  and  $30\text{ }\mu\text{m}$ , respectively. The laser pulses consisted of a prepulse and a main pulse with durations of  $200\text{ ps}$  and  $7\text{ ps}$ , separated by  $250\text{ ps}$ . The intensity on the target was  $3.0 \times 10^{12}\text{ W/cm}^2$  for the prepulse and  $1.4 \times 10^{15}\text{ W/cm}^2$  for the main pulse. We employed a quasitraveling wave pumping by use of a step mirror with a step of  $4\text{ ps}$  [4]. The emission from the La plasma was observed using a grazing incidence spectrograph, GIS1, and a potassium acid phosphate (KAP) crystal spectrograph (KAPCS). GIS1, which had a concave collecting mirror and uneven spacing grating ( $1200\text{ l/mm}$ ) [17], covered spectral range of  $6\text{--}40\text{ nm}$  and was set in the propagation direction of x-ray laser beam. In order to attenuate the emission from the plasma, we used a Zr filter with a transmittance of  $10\%$  at  $8.8\text{ nm}$ . KAPCS was set at the top port of the chamber and observed the plasma in the downward direction. It covered  $0.8\text{--}1.0\text{ nm}$  and the  $n=3\text{--}5$  transitions of the Ni-, Co-, and Fe-like La ions were observed. The detectors of these spectrographs were back-illuminated CCD (charge-coupled device, Princeton instrument Model SX1024). The wavelength calibration of GIS1 was done by use of the second- and third-order light of resonance lines of H-like C ions. For KAPCS, we used resonance series lines of the He-like Na ions. By use of this calibration curve together with the theoretical wavelengths calculated by the HULLAC code [18], several lines of the Ni-, Co-, and Fe-like La ions taken by KAPCS were identified as a spectral evidence of these ions.

Figures 1(a) and 1(b) show the spectra taken by GIS1 for the target lengths of  $5.3\text{ mm}$  and  $2.6\text{ mm}$ , and the spectrum taken by KAPCS, respectively. The lasing line and the resonance lines of the Ni-, Co-, and Fe-like ions are marked by arrows. Substantial amplification of the  $8.8\text{-nm}$  line of the Ni-like La ions is obvious. In this target shot, the energies of the prepulse and main pulse were  $1\text{ J}$  and  $17\text{ J}$ , respectively. Figure 2 shows the output of the  $8.8\text{-nm}$  line versus various target lengths. The gain coefficient  $g$  and gain-length product  $gl$  were derived to be  $14.5 \pm 1.5\text{ cm}^{-1}$  and  $gl = 7.7 \pm 0.8$ , respectively, by use of the Linford fitting formula [19].

We observed the dependence of the output of the  $8.8\text{-nm}$  line on the prepulse intensity. The main-pulse energy was fixed to be  $17\text{ J}$ , and the prepulse intensity was changed from  $5 \times 10^{11}$  through  $1.2 \times 10^{13}\text{ W/cm}^2$ . Figure 3 shows the result. The abscissa is the intensity (or energy) of the prepulse, and the closed circles represent the output of the  $8.8\text{-nm}$  line, which is referred to the left-hand-side ordinate. The  $8.8\text{-nm}$  output has a peak at around prepulse intensity of  $3 \times 10^{12}\text{ W/cm}^2$ . The open triangles and open diamonds represent the line intensity ratios,  $r_1$  and  $r_2$ , of the  $3d\text{--}5f$  lines of the Ni-like ( $0.95\text{ nm}$ ), Co-like ( $0.91\text{ nm}$ ), and Fe-like ions ( $0.86\text{ nm}$ ), i.e.,  $r_1 = I(\text{Co-like})/I(\text{Ni-like})$  and  $r_2 = I(\text{Fe-like})/I(\text{Ni-like})$ , respectively. The increase of these intensity ratios corresponds to the increase of the electron temperature.

In the prepulse intensity region of  $1 \times 10^{12}\text{--}1.2 \times 10^{13}\text{ W/cm}^2$ , the  $r_1$  and  $r_2$  increase with decrease of the

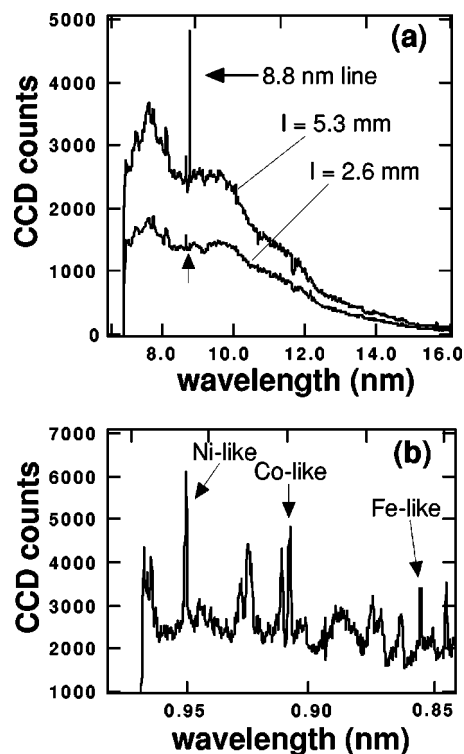


FIG. 1. (a) Typical spectra of the Ni-like La lasing line taken by GIS1. The target length was  $5.3\text{ mm}$  and  $2.6\text{ mm}$ . The lasing line is indicated by an arrow. (b) Typical spectrum of the La plasma taken by KAPCS. A few lines of the Ni-, Co-, and Fe-like ions are indicated by arrows.

prepulse intensity. This indicates that by reducing the prepulse intensity, the volume of the preformed plasma is reduced, and the main pulse energy is absorbed in a localized area. The localized heating is reproduced by one-dimensional hydrodynamics calculation using HYADES [20] in which the heat conduction is treated by the classical flux corrected Spitzer-Härm method. In the present calculation typical value of the flux limiter is  $0.4$ . Figure 4 shows the temporal evolution of the spatial profile of  $T_e$  under the laser irradiation.

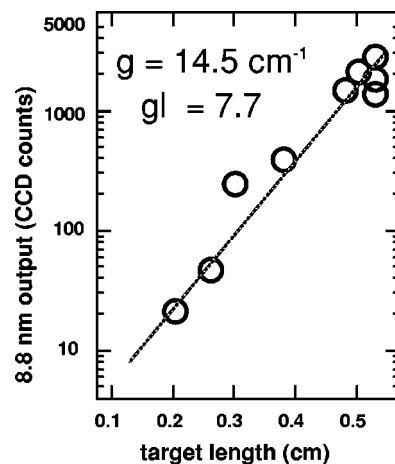


FIG. 2. The output of the  $8.8\text{-nm}$  line for various target lengths. Gain coefficient was estimated to be  $\sim 14.5 \pm 1.5\text{ cm}^{-1}$ , and the achieved  $gl$  was  $7.7 \pm 0.8$ .

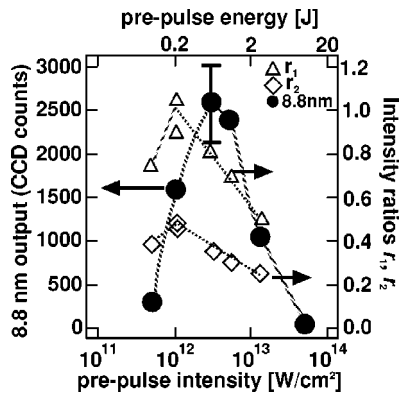


FIG. 3. The prepulse dependence of the output of the 8.8-nm line. The main pulse energy was fixed to be 17 J. The closed circle is the 8.8-nm line output (the left-hand-side ordinate). The open circle and triangle are the intensity ratio of Co-like/Ni-like ( $=r_1$ ) and Fe-like/Ni-like ( $=r_2$ ), respectively (right-hand side ordinate).

tion condition similar to the experiment. The time is measured from the peak of the prepulse. The prepulse intensity is (a)  $1 \times 10^{12}$  and (b)  $4 \times 10^{12}$  W/cm<sup>2</sup>, and the main pulse intensity is fixed to be  $5 \times 10^{14}$  W/cm<sup>2</sup>. After the main pulse irradiation (see the trace for 300 ps), the size of the high-temperature region in Fig. 4(a) is smaller than that in Fig. 4(b), and the peak value of  $T_e$  becomes higher with decreasing the prepulse intensity. The effect of the nonlocal heat transport is discussed below.

In order to calculate the spatial gain profile, we performed our collisional-radiative model code (WHIAM [21]) for given spatial profile of electron density and temperature. The atomic data employed in the WHIAM code were calculated by HULLAC code. In the present condition of experiment, the Doppler width and Stark width are comparable which dominate the total spectral profile. Thus, the width was treated as a Voigt profile. The ion temperature was calculated by HYADES, and the collisional-radiative destruction rate was cal-

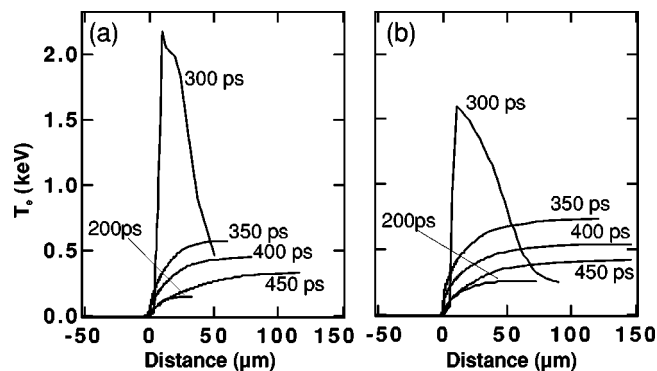


FIG. 4. Temporal evolution of the spatial profiles of  $T_e$  under a condition similar to the present experiment. The time is measured from the peak of the prepulse, and the main pulse reaches the preformed plasma at 250 ps. The abscissa is the position from the target surface. The prepulse intensity is (a)  $1 \times 10^{12}$  and (b)  $4 \times 10^{12}$  W/cm<sup>2</sup>, and the main pulse intensity is fixed to be  $5 \times 10^{14}$  W/cm<sup>2</sup>. By reducing prepulse intensity, the main pulse energy is absorbed in a localized area, the size of the heated area becomes smaller, and the peak temperature becomes higher.

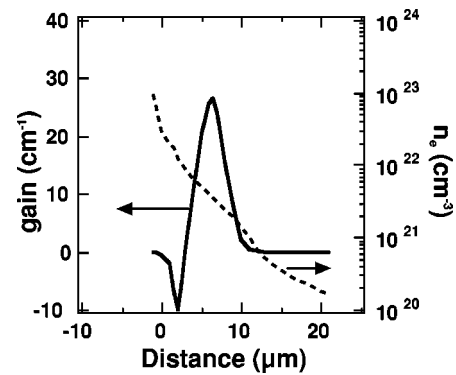


FIG. 5. The spatial profile of the electron density (dotted line) and the gain of the 8.8-nm line (solid line) at 300 ps under the condition of Fig. 4(a).

culated by HULLAC code; typically they were  $1.60 \times 10^{13}$  s<sup>-1</sup> (upper level) and  $1.32 \times 10^{13}$  s<sup>-1</sup> (lower level) under the condition of  $n_e = 3 \times 10^{21}$  cm<sup>-3</sup>,  $T_e \sim 1$  KeV, and  $T_i \sim 400$  eV. This lead to the full width at half maximum of the Gaussian profile of 11.7 mÅ and that of the Lorentzian of 12.1 mÅ. Figure 5 shows the spatial profile of the gain of the 8.8 nm and the electron density at 300 ps under the condition of Fig. 4(a). The peak gain is obtained in the overdense region ( $\sim 3 \times 10^{21}$  cm<sup>-3</sup>). The value of the calculated gain is larger by a factor of 2 than the experimental gain, which may be due to the fact that the experimental gain is spatially averaged one.

The calculated results imply that the overdense region can be heated effectively by the electron thermal conduction as shown in Figs. 4 and 5. On the other hand, one may expect that the heat conduction inside the plasma with a steep gradient leads to the nonlocal heat transport. The effect of the nonlocal electron heat transport has also been experimentally investigated by Coté *et al.* [22], and they have shown that it becomes substantial if the scale length is comparable to the wavelength of the pumping laser. However, under the present situation, the scale length of the preformed plasma is much longer than the wavelength of the pump laser, and the gain is generated in lower density region than that of the heat front. Thus, the effect of the nonlocal heat transport is small in the present case. Indeed, calculations with various flux limiter values from 0.07 to 0.6 are also carried out to find that the gain is insensitive to the change of the flux limiter: The change of time of the gain peak was less than 10 ps and that of the gain coefficient was around 10%.

At the prepulse intensity of  $1 \times 10^{12}$  W/cm<sup>2</sup>, Fig. 3 shows that the x-ray output becomes small compared with the peak value although the  $r_1$  and  $r_2$  values increase. This may be due to the refraction of the amplified x ray in the gain medium. Qualitative estimation of the propagation length  $l_p$  of the 8.8-nm line in the gain region indicates  $l_p = [2n_c d / \text{grad}(n_e)]^{1/2} \sim 1$  mm, the same order as the target length, where  $n_c = 1.4 \times 10^{25}$  cm<sup>-3</sup> for the 8.8 nm, and the size of the gain region ( $d = 10$  μm) and the density gradient [ $\text{grad}(n_e) \sim 2 \times 10^{24}$  cm<sup>-4</sup>] are estimated from Fig. 5. This means that the x-ray beam propagation is sensitive to the prepulse intensity in the present case, and in order to achieve more efficient lasing at this wavelength we have to compen-

sate the refraction by use of additional means such as curved targets [23]. On the other hand, at the prepulse intensity smaller than  $1 \times 10^{12}$  W/cm<sup>2</sup>,  $r_1$  and  $r_2$  decrease, showing the decrease in the absorption efficiency of the main pulse due to the insufficient generation of the preformed plasma.

In order to increase the peak intensity of the main pulse, we changed the duration of the main pulse into 1 ps under the prepulse intensity of  $3 \times 10^{12}$  W/cm<sup>2</sup>. However, the output of the 8.8-nm line became smaller by a factor of 4 compared with the 7-ps-duration case. This is due to the following. Under the present prepulse intensity of the order of  $10^{12}$  W/cm<sup>2</sup>, the observation of the preformed plasma by use of the KAPCS shows that the La ions are populated in the lower ionization stage than the Ni-like ions. Under such a condition, the main pulse has to sustain high temperature

during the ionization from the lower ionization stages to the Ni-like ions. This is consistent with the calculated ionization time from La<sup>28+</sup> to La<sup>29+</sup> of  $\sim 10$  ps by use of WHIAM code together with HYADES.

In summary, we have demonstrated substantial amplification of 8.8-nm line in the transient collisional-excitation scheme with a pumping energy of 18 J. The present result suggests that the overcritical density region can be heated enough to generate substantial population inversion by control of the scale length of the preformed plasma and is valuable in terms of development of highly efficient x-ray lasers in a shorter wavelength region.

The authors are grateful to Professor T. Tajima of JAERI for his useful suggestions.

- 
- [1] M. P. Kalachnikov, P. V. Nickles, M. Schnürer, W. Sandner, V. N. Shlyatsev, C. Danson, D. Neely, E. Wolftrum, J. Zhang, A. Behjat, A. Demir, G. J. Tallents, P. J. Warwick, and C. L. S. Lewis, *Phys. Rev. A* **57**, 4778 (1998).
- [2] J. Dunn, A. L. Osterheld, J. Nilsen, J. R. Hunter, and V. N. Shlyaptsev, *Phys. Rev. Lett.* **84**, 4834 (2000).
- [3] A. Klisnick, P. Zeitoun, D. Ros, A. Carillon, P. Fourcade, S. Hubert, G. Jamelot, C. L. S. Lewis, A. MacPhee, R. O'Rourke, R. Keenan, P. Nickles, K. Janulewicz, M. Kalachnikov, J. Warwick, J. C. Chanteloup, A. Migus, E. Salmon, C. Sauteret, and J. P. Zou, *J. Opt. Soc. Am. B* **17**, 1093 (2000).
- [4] T. Kawachi, M. Kado, M. Tanaka, A. Sasaki, N. Hasegawa, A. V. Kilpio, S. Namba, K. Nagashima, P. Lu, K. Takahashi, H. Tang, R. Tai, M. Kishimoto, M. Koike, H. Daido, and Y. Kato, *Phys. Rev. A* **66**, 033815 (2002).
- [5] H. Daido, Y. Kato, K. Murai, S. Ninomiya, R. Kodama, G. Yuan, Y. Oshikane, M. Takagi, H. Takabe, and F. Koike, *Phys. Rev. Lett.* **75**, 1074 (1995).
- [6] R. E. King, G. J. Pert, S. P. McCabe, P. A. Simms, A. G. MacPhee, C. L. S. Lewis, R. Keenan, R. M. N. O'Rourke, G. J. Tallents, S. J. Pestehe, F. Strati, D. Neely, and R. Allott, *Phys. Rev. A* **64**, 053810 (2001).
- [7] J. Zhang, A. G. MacPhee, J. Lin, E. Wolftrum, R. Smith, C. Danson, M. H. Key, C. L. S. Lewis, D. Neely, J. Nilsen, G. J. Pert, G. J. Tallent, and J. S. Wark, *Science* **276**, 1097 (1997).
- [8] R. Tai, K. Namikawa, M. Kishimoto, M. Tanaka, K. Sukegawa, N. Hasegawa, T. Kawachi, M. Kado, P. Lu, K. Nagashima, H. Daido, H. Maruyama, A. Sawada, M. Ando, and Y. Kato, *Phys. Rev. Lett.* **89**, 257602 (2002).
- [9] S. B. Da Silva, J. E. Trebes, R. Balhorn, S. Mrowka, E. Anderson, D. T. Attwood, T. W. Barbee, Jr., J. Brase, M. Corzett, J. Gray, J. A. Koch, C. Lee, D. Kern, R. A. London, B. J. MacGowan, D. L. Matthews, and G. Stone, *Science* **258**, 269 (1992).
- [10] P. J. Warwick, C. L. S. Lewis, S. MacCabe, A. G. MacPhee, A. Behjat, M. Kurcuoglu, G. J. Tallents, D. Neely, E. Wolftrum, S. B. Healy, and G. J. Pert, *Opt. Commun.* **144**, 192 (1997).
- [11] J. Nilsen, B. J. MacGowan, L. B. Da Silva, and J. C. Moreno, *Phys. Rev. A* **48**, 4682 (1993); J. Nilsen and J. C. Moreno, *Phys. Rev. Lett.* **74**, 3376 (1995).
- [12] R. C. Elton, *X-Ray Lasers* (Academic Press, New York, 1990).
- [13] T. Fujimoto, *J. Phys. Soc. Jpn.* **54**, 2905 (1980).
- [14] J. Nilsen, Y. Li, J. Dunn and A. L. Osterheld, in *Proceedings of X-ray Lasers—1998*, edited by Y. Kato, H. Takuma, and H. Daido, IOP Conf. Proc. No. 159 (Institute of Physics, Bristol 1998), p. 135.
- [15] B. J. MacGowan, S. Maxon, L. B. DaSilva, D. J. Foelds, D. C. Keane, A. L. Matthews, A. L. Osterheld, J. H. Scofield, G. Shimkaveg, and G. F. Stone, *Phys. Rev. Lett.* **65**, 420 (1990).
- [16] T. Kawachi, M. Kado, M. Tanaka, N. Hasegawa, K. Nagashima, K. Sukegawa, P. Lu, K. Takahashi, S. Namba, M. Koike, A. Nagashima, and Y. Kato, *Appl. Opt.* **42**, 2198 (2003).
- [17] M. Koike, T. Namioka, E. Gullikson, Y. Harada, S. Ishikawa, T. Imazono, S. Mrowka, N. Miyata, M. Yanagihara, J. H. Underwood, K. Sano, N. Ogiwara, O. Yoda, and S. Nagai, *Proc. SPIE* **4146**, 163 (2000).
- [18] M. Klapisch and A. Bar-Shalom, *J. Quant. Spectrosc. Radiat. Transf.* **58**, 687 (1997).
- [19] G. J. Linford, E. P. Poressini, W. R. Sooy, and M. L. Spaeth, *Appl. Opt.* **13**, 379 (1974).
- [20] J. T. Larsen and S. M. Lane, *J. Quant. Spectrosc. Radiat. Transf.* **51**, 179 (1994).
- [21] A. Sasaki, T. Utsumi, K. Moribayashi, M. Kado, M. Tanaka, N. Hasegawa, T. Kawachi, and H. Daido, *J. Quant. Spectrosc. Radiat. Transf.* **71**, 665 (2001).
- [22] C. Y. Coté, J. C. Kieffer, and O. Peyrusse, *Phys. Rev. E* **56**, 992 (1997).
- [23] R. Kodama, D. Neely, Y. Kato, H. Daido, K. Murai, G. Yuan, A. G. MacPhee, and C. L. S. Lewis, *Phys. Rev. Lett.* **73**, 3215 (1994).